Micro- and Macrorheology of Jellyfish Extracellular Matrix

Camille Gambini, Bérengère Abou, Alain Ponton, and Annemiek J. M. Cornelissen*
Laboratoire Matière et Systèmes Complexes, UMR 7057, Université Paris Diderot, Sorbonne Paris Cité, Paris, France

ABSTRACT Mechanical properties of the extracellular matrix (ECM) play a key role in tissue organization and morphogenesis. Rheological properties of jellyfish ECM (mesoglea) were measured in vivo at the cellular scale by passive microrheology techniques: microbeads were injected in jellyfish ECM and their Brownian motion was recorded to determine the mechanical properties of the surrounding medium. Microrheology results were compared with macrorheological measurements performed with a shear rheometer on slices of jellyfish mesoglea. We found that the ECM behaved as a viscoelastic gel at the macroscopic scale and as a much softer and heterogeneous viscoelastic structure at the microscopic scale. The fibrous architecture of the mesoglea, as observed by differential interference contrast and scanning electron microscopy, was in accord with these scale-dependent mechanical properties. Furthermore, the evolution of the mechanical properties of the ECM during aging was investigated by measuring microrheological properties at different jellyfish sizes. We measured that the ECM in adult jellyfish was locally stiffer than in juvenile ones. We argue that this stiffening is a consequence of local aggregations of fibers occurring gradually during aging of the jellyfish mesoglea and is enhanced by repetitive muscular contractions of the jellyfish.

INTRODUCTION

The extracellular matrix (ECM) provides structural scaffolding for cellular organization and strongly influences the functional behaviors of resident cells by biochemical and mechanical interactions. Thus, the mechanical and viscoelastic properties of the ECM play a crucial role in cell behaviors, tissue organization, morphogenesis, and development (1–5).

In our search to understand the morphogenesis of the endodermal gastrovascular system of jellyfish, the architecture and the mechanical properties of the ECM (mesoglea) surrounding this tissue are of special interest.

Jellyfish are particularly well suited to the study of in vivo mechanical properties of the ECM. Indeed, the ECM is the most prominent structure in jellyfish, with some jellyfish being transparent such as the widespread common jellyfish *Aurelia aurita* (Scyphozoa, Cnidaria). Such transparency enables us to easily study its ECM by microscopy techniques.

In jellyfish, the mesoglea is an extracellular substance situated between the epidermal and endodermal layers. It is a highly hydrated fibrous substance containing mucopolysaccharides (6), collagen fibrils (6–10), microfibrils rich in protein homologous to mammalian fibrillins (11), and other structural proteins. Its stiffness is provided by collagen fibrils and its elasticity by fibrillin microfibrils (12). Mesoglea of some jellyfish species, as *A. aurita*, contain mesogleal cells, which are free motile cells involved in the formation of mesogleal fibers (13).

The ECM of jellyfish performs important functions. As in vertebrates, its elementary function is to serve as a base for cell attachment to maintain the animal body structure (6). It is also involved in the transport and storage of nutrients (6) and in buoyancy regulation (14). The fiber architecture of the mesoglea is constructed in close functional relation to the locomotory system of the jellyfish (15). Moreover, recent studies proved that jellyfish locomotion and morphogenesis are tightly linked (16,17). Because jellyfish has no antagonist muscle, recovery after muscle contraction is affected by the ECM: its elasticity allows passive release of the energy stored during the contracted state (8,12,18). Finally, the mesoglea plays an important role in control of cellular migration and differentiation and morphogenetic processes (19–24).

Many studies have been conducted on the chemical composition, architecture, and role of the mesogleal ECM, but there are few measurements of its mechanical properties and these measurements were always performed at the macroscopic scale: Alexander (25) studied the creep response of mesoglea, and Megill et al. (12) its compressive stiffness. However, to study the role of the mechanical properties of ECM in cellular migration and morphogenesis, mechanical measurements have to be performed locally, at the cellular scale. In recent years, microrheology techniques have shown to be powerful ways to probe the viscoelastic properties of soft and biological materials at the micron scale (26,27). These methods enable us to study mechanical properties of small biological samples (28), including living cells (29–32), and allow measurements of heterogeneities through the sample (33,34). Microrheology techniques involve the use of microprobes to measure the relation between stress (probe force) and deformation (probe position) at the microscopic scale. Various techniques can be used to apply the force, like manipulation of magnetic beads (35) or laser-trap microrheometry techniques (36). Instead of using an external excitation to move the probes, the intrinsic Brownian motion of the particles can be used (37). In this

Submitted July 21, 2011, and accepted for publication November 28, 2011.

*Correspondence: annemiek.cornelissen@univ-paris-diderot.fr

Editor: Charles Wolgemuth.

0006-3495/12/01/0001/9 $2.00

doi: 10.1016/j.bpj.2011.11.4004

case, the driving force is thermal. The probe position can be measured by video microscopy (28) or dynamic light scattering techniques (37,38).

In this article, we measure the mechanical properties of the ECM by injecting microbeads and subsequently tracking their Brownian motion by video microscopy techniques. The driving force is thermal, with an energy scale corresponding to k_BT, with k_B being the Boltzmann constant and T the absolute temperature. Because this driving force is small, only the linear viscoelastic response of the sample is probed. Measurements of the particles' mean-squared displacement (MSD) through particle tracking give access to the local elastic (G') and viscous (G'') moduli of the embedding medium (39). In addition, rheological measurements are performed at a macroscopic scale with a shear rheometer. The fibrous architecture of the mesoglea observed by differential interference contrast (DIC) and scanning electron microscopy (SEM) is in accordance with our measurements of the mechanical properties of the ECM at macroscopic and microscopic scales. Furthermore, we investigate the evolution of the mechanical properties of the ECM during aging in performing microrheological measurements at different stages of jellyfish development.

MATERIAL AND METHODS

Jellyfish culture

Jellyfish *A. aurita* were reared in the laboratory, at room temperature, in artificial seawater, produced by diluting 40 g of synthetic sea salt (Instant Ocean; Spectrum Brands, Madison, WI) per liter of osmosis water (osmolarity 1100 mOsm). Strobilation in polyps was induced by a lowering of temperature down to 10°C (40). The newborn ephyrae were bred to adult stage.

The measurements were performed on jellyfish at different developmental stages: juvenile or adult jellyfish. Juvenile jellyfish had just reached the circular shape of adult medusas with a diameter of ~1 cm. Adult jellyfish were at a much later developmental stage (several months) with a diameter of ~10 cm.

Visualization of the thick fibers in the mesoglea

Slices of mesoglea were cut from adult jellyfish and the organization of their fibers was revealed using DIC microscopy (inverted microscope DMI 3000 B; Leica, Nanterre, France, with objective PL Fluotar 20×/0.40 Corr; also Leica). Images were recorded with a camera (CFW-1612M; Scion, Frederick, MD) controlled by ImageJ software (National Institutes of Health, Bethesda, MD). The slices of mesoglea were either cut lateral along the oral-aboral axis, ~1–2 mm above the endoderm, to visualize the thick vertical fibers, or perpendicularly to the oral-aboral axis, ~10 μm under the exumbrella, to see the plexus of thick tangential fibers (Fig. 1).

Scanning electron microscopy experiments

For SEM experiments, juvenile jellyfish and pieces of mesoglea cut from adult jellyfish were fixed overnight in 5% glutaraldehyde (Cat. No. 49626; Sigma, Saint-Quentin-Fallavier, France) in 0.1 M cacodylate buffer (Cat. No. C4945; Sigma) (41). They were rinsed in 0.5 M cacodylate buffer,

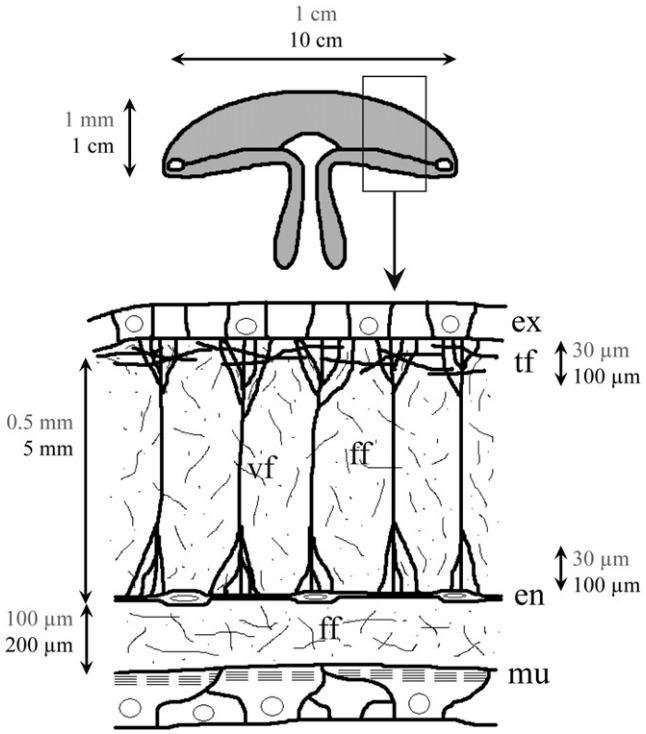

FIGURE 1 Schematic view of the fibrous network organization of mesoglea of *A. aurita*. For clarity, the diagram does not show actual sizes of the various structures. (*Vertical arrows*) Direction of the oral-aboral axis. Characteristic length-scales of jellyfish and mesogleal fibrous architecture network for adult jellyfish (*solid*) and juvenile jellyfish (*shaded*). Visualizations by DIC microscopy of the thick vertical and tangential fibers are shown in Fig. 2, *A* and *B*, respectively. Visualizations by SEM microscopy of the fine fibers are shown in Fig. 3. Endoderm (*en*); exumbrella (*ex*); fine fibers (*ff*); subumbrellar swimming muscle (*mu*); thick tangential fibers (*tf*); thick vertical fibers (*vf*). Figure adapted from Weber and Schmid (15).

dehydrated with acetone, and critical-point-dried with CO_2. To best preserve the biological structures, the osmolarity of the fixative and rinsing solutions were verified to be close to the seawater osmolarity (42). To visualize the internal structure of the mesoglea, the skin of the critical-point-dried specimen was carefully lifted at different places with a fine needle to observe the fibrous network ~100–400 μm above the endoderm. The specimens were then coated with platinum. The observations were performed with a field emission scanning electron microscope (SUPRA 40; Carl Zeiss, Nanterre, France).

Macrorheology experiments

For the macrorheology experiments, cylindrical slices of mesoglea (diameter 25 mm and height 2 mm, perpendicular to the oral-aboral axis) were cut from adult jellyfish, far from cellular sheets and tangential big fibers. The measurements were performed with a controlled-strain rheometer (ARES G2; TA instruments, Guyancourt, France), at 20°C, with parallel-plate geometry (diameter 25 mm; gap 2 mm). To avoid any sliding of the sample, rough plates were used and a constant normal force was applied during the measurement. Sample evaporation was minimized using a solvent trap.

The elastic (G') and viscous (G'') moduli were measured by imposing sinusoidal strains and measuring resulting stresses. The linearity of the sample was checked by measuring G' and G'' with sinusoidal strains at fixed frequency ($f = 1$ Hz) and increasing strain amplitudes from 0.01 to 100%.

The samples of mesoglea were linear up to 1% strain amplitude. The frequency dependence of the moduli G' and G'' was measured in the linear viscoelastic range by varying the frequency between 0.13 and 20 rad/s at a constant strain amplitude set to 0.3%.

Microrheology experiments on juvenile jellyfish

Suspensions of yellow green amine-modified fluorescent microspheres with a diameter of 1 μm (F8765; Invitrogen, Cergy-Pontoise, France) were prepared at a concentration of 10^8 particles/ml of artificial seawater.

Details of the injection and microrheology experimental procedure are described in the Supporting Material.

In short, a few nanoliters of microbead suspension were injected ~200 μm above the subumbrella so that the microbeads were well embedded in the mesoglea far from cellular sheets, but could be visualized in vivo to track their Brownian motion.

After injection, jellyfish were replaced in artificial seawater, where they swam freely during one day before any measurement of the motion of the beads. It was verified that diffusion of the injected seawater and local embedding of each bead in the mesogleal fibrous network were well achieved one day after injection. We also verified that the microinjection process did not affect normal morphology and behavior of the jellyfish.

For the microrheological measurements, the jellyfish were put on a glass coverslip, in the same position as for the injection: the umbrella was lying flat and the subumbrella was in contact with the coverslip (see Fig. S1). The thermal motion of the microbeads in the ECM was recorded at room temperature ($T = 21 \pm 2°C$), with bright light, using the ×63 glycerine immersion objective, coupled to a CMOS camera (Fastcam-Ultima 1024; Photron, Marly-le-Roi, France). Beads phagocytized by mesogleal cells are ignored. Images were acquired at 500 frames/s during 8 s, with a $100 \times 100\ \mu m^2$ field of view. Depending on the realization, 5–30 microbeads could be recorded in the same field of view. A home-made analysis software (43) allowed us to track the bead positions $x(t)$ and $y(t)$. To increase signal/noise ratio, we only tracked microbeads moving in the focus plane of the objective.

After drift-correction of the beads positions, the time-averaged two-dimensional MSD $\langle \Delta r^2(t) \rangle_{t'} = \langle [x(t'+t) - x(t')]^2 + [y(t'+t) - y(t')]^2 \rangle_{t'}$ was calculated for each bead, improving the statistical accuracy. To maintain reliable statistics, the data from the MSD were kept in the range $t < 2$ s.

Microrheology experiments on adult jellyfish

Microrheology experiments were also performed on adult jellyfish. As they are much bigger (10 cm in diameter) than juvenile ones, slices of their mesoglea were hand-cut, far from cellular sheets and tangential large fibers (~1–2 mm above the endoderm). The experiments were performed on these slices similarly as in vivo measurements described above.

No muscle fibers were present on these slices and therefore it was not necessary to anesthetize the samples in $MgCl_2$. After injection of the fluorescent microbeads, the samples were stored one day in a fridge at 7°C, to preserve them from bacteria and to allow equilibration between bead suspension and ECM. We verified that the microinjection and the storage at low temperature did not affect the shape of the sample and the behavior of the mesogleal cells; at low temperature, the samples were well preserved for several weeks, as also reported in Weber et al. (44). As for the juvenile jellyfish, the thermal motion of the microbeads was recorded at room temperature, the drift corrected, and the MSD calculated for each bead.

Control experiments

Microrheology experiments in calibrated glycerol solutions were performed under similar conditions to verify whether the experimental setup and statistics applied are reliable. To rule out a systematic bias in bead distributions, microrheological experiments were repeated in juvenile jellyfish under the same experimental conditions as for adult jellyfish. To exclude that the differences observed between juvenile and adult jellyfish are due to the chemical interactions of the bead surface groups with its environment, microrheology control experiments were also performed with polystyrene microbeads.

These control experiments are presented in the Supporting Material.

Viscoelastic moduli from particle tracking

To compare microrheological with macrorheological measurements, the frequency-dependent elastic modulus $G'(\omega)$ and viscous modulus $G''(\omega)$ were computed from the measured MSD. The frequency dependence of the viscoelastic moduli is obtained from the two-dimensional MSD by using the generalized Stokes-Einstein relation (37,39,45),

$$G(s) = \frac{k_B T}{\pi R s \frac{3}{2} \langle \Delta r^2(s) \rangle}, \quad (1)$$

where k_B is the Boltzmann constant, T the temperature, R the microbead radius, s the Laplace frequency, $\langle \Delta r^2(s) \rangle$ the Laplace transform of the MSD, and $G(s)$ the complex viscoelastic modulus in the Laplace domain. In Eq. 1, the factor 3/2 is a dimensional correction: the three-dimensional MSD is simply calculated from the two-dimensional MSD by multiplying the latter by 3/2, assuming that the medium surrounding locally each bead is isotropic (27). The generalized Stokes-Einstein relation (Eq. 1) can be obtained from a generalized Langevin model equation, assuming moreover that the Stokes relation can be generalized to viscoelastic fluids with a frequency-dependent linear viscoelastic modulus and that inertial effects are negligible (27,39).

The viscoelastic moduli can be obtained from the dynamics of the probe particles assuming that the MSD of the beads can be described by a local power law (39). This method, valid for MSD curves changing slowly, eschews any Laplace transformation of MSD (Eq. 1); resulting truncation errors introduced by numerical transformation of data over a limited range; and the use of any arbitrary functional form to fit $G(s)$ (39,46). The power law behavior is determined from the logarithmic time derivative of the MSD. For thermally driven microbeads, the slope of the logarithmic time derivative of the MSD lies between zero, corresponding to elastic confinement, and one, corresponding to viscous diffusion (39,46). Assuming a local power law form for MSD, elastic $G'(\omega)$ and viscous $G''(\omega)$ moduli are given by (39,46)

$$G'(\omega) = G(\omega) \cos\left[\frac{\pi \alpha(\omega)}{2}\right], \quad (2)$$

$$G''(\omega) = G(\omega) \sin\left[\frac{\pi \alpha(\omega)}{2}\right], \quad (3)$$

where

$$G(\omega) = \frac{2 k_B T}{3 \pi R \langle \Delta r^2(1/\omega) \rangle \Gamma[1 + \alpha(\omega)]}. \quad (4)$$

In Eq. 4, $\langle \Delta r^2(1/\omega) \rangle$ is the magnitude of $\langle \Delta r^2(t) \rangle$ evaluated at $t = 1/\omega$. The value Γ denotes the γ-function. The value $\alpha(\omega)$ is the exponent of the local power law, determined from the logarithmic time derivative of the MSD: $\alpha(\omega) = \partial \mathrm{In}[\langle \Delta r^2(t) \rangle] / \partial \mathrm{In}[t]|_{t = 1/\omega}$.

RESULTS

Visualization of the thick fibers in the mesoglea

The thick vertical fibers could easily be revealed by DIC microscopy in hand-cut sections of outer mesoglea (mesoglea

between the endoderm and the exumbrella). The outer mesoglea is traversed by radially arranged fibers, as described in other species of jellyfish (7,12,15,18). Weber and Schmid (15) described in detail the fibrous system of the ECM of hydromedusa *Polyorchis penicillatus*. We found the same architecture of the fibrous system in adult *A. aurita* (Fig. 1): thick vertical fibers run perpendicularly from the exumbrellar side and impinge on the endoderm (Fig. 2 *A*) and near the exumbrellar surface the fibers branch and penetrate a plexus of fibers that run tangentially in all directions (Fig. 2 *B*). In juveniles the resolution of DIC microscopy was too low, but we could occasionally observe in vivo parts of the thick fiber structures. In Fig. 2, *A* and *B*, apart from the thick fibers, many mesogleal cells, randomly distributed, can be observed. The thick fibers vary in diameter (up to 12 μm). They are anchored in a three-dimensional network of fine fibrils that fills the entire volume of the mesogleal ECM. This fine fibrous structure is transparent by light microscopy but can be revealed by SEM.

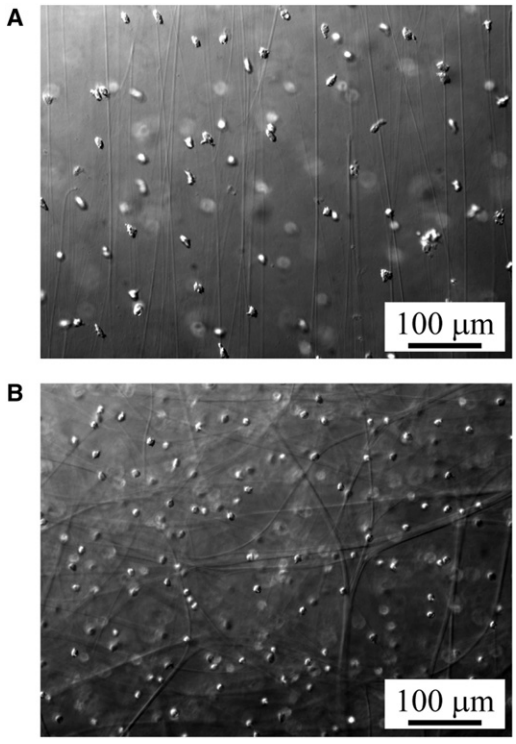

FIGURE 2 Thick fibers of the ECM. Hand-cut sections of adult jellyfish mesoglea were visualized by DIC microscopy. The thick fibers of the ECM and numerous randomly distributed mesogleal cells can be observed. (*A*) Thick vertical fibers and mesogleal cells. The slice of mesoglea was cut lateral along the oral-aboral axis, in the middle of the mesoglea, ~1–2 mm above the endoderm. The thick vertical fibers are parallel and run perpendicularly from the exumbrellar side. (*B*) Thick tangential fibers and mesogleal cells. The slice of mesoglea was cut perpendicularly to the oral-aboral axis, ~10 μm under the exumbrella. The thick tangential fibers run tangentially in all directions, near the exumbrellar surface.

Visualization of the fine fibers in the mesoglea

Because of the large quantity of water in the mesoglea, the samples underwent a noticeable shrinkage (with a ratio of ~2) occurring during fixation, dehydration, and especially during critical-point drying. For this reason, the mesh size of the mesogleal fibrous network may be smaller in SEM observations than in vivo and the fiber diameters might be slightly smaller (47,48). However, we assume that SEM observations gave reliable information on fiber structure and architecture of the fibrous network (15).

Fig. 3, *A* and *B*, shows the structure of the mesoglea of juvenile jellyfish visualized by SEM, in the thick vertical fibers region. As can be observed in Fig. 3 *A*, the thick fibers stick out of the network of fine fibrils and are woven together by many fibrils of the three-dimensional network; this was also observed by Weber and Schmid (15) in *P. penicillatus*. Fig. 3 *B* shows a mesogleal cell embedded in the fine network of fibrils. The SEM images show that the fibrils are randomly and heterogeneously distributed. Moreover, the size of the fibrous mesh is variable. A similar fibrous organization was observed on pieces of mesoglea cut from adult jellyfish.

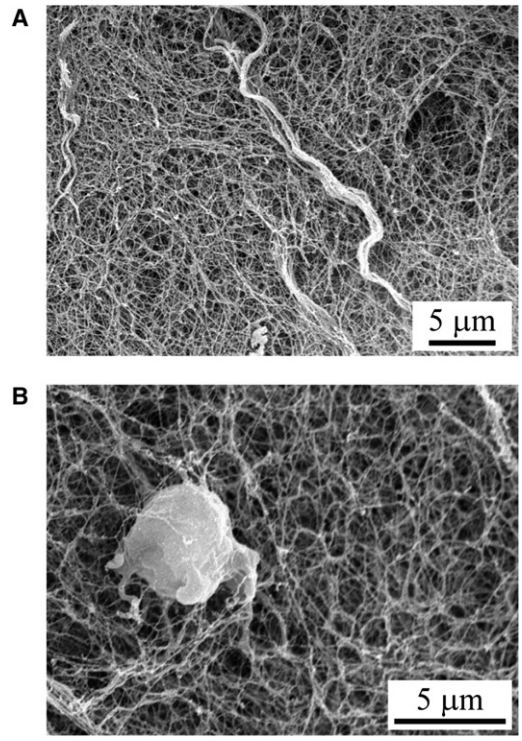

FIGURE 3 Scanning electron micrographs of the mesoglea of juvenile jellyfish in the middle of the mesoglea, ~100–400 μm above the endoderm. (*A*) Thick fibers emerging from the three-dimensional network of fine fibrils. The thick fibers are woven together by many fibrils of the three-dimensional network. The fibrils are randomly and heterogeneously distributed and the size of the fibrous mesh is very variable. A similar fibrous organization was observed on pieces of mesoglea cut from adult jellyfish. (*B*) A mesogleal cell embedded in the fine network of fibrils.

Macrorheology experiments

The experiments were performed on 18 different slices of mesoglea, cut from six different adult jellyfish. All the slices were extracted from the same functional network region, characterized by the thick vertical fibers architecture.

The frequency dependence of the elastic (G') and viscous (G'') moduli was obtained by measuring the stress response from sinusoidal strain variations (amplitude 0.3%) with frequencies varying from 0.13 to 20 rad/s. Each sample showed the same kind of behavior: G' was higher than G'', and G' slightly increased with frequency. We observed a relatively small sample-to-sample variation in the measurements of elastic and viscous moduli. The averaged viscous and elastic moduli (averaged over the 18 samples) were plotted as a function of frequency (Fig. 4); the bars represent the standard deviation. The observed frequency dependence of the viscoelastic moduli shows that the mesoglea behaves like a viscoelastic material (36). Between 1 and 20 rad/s, G' and G'' increase with frequency with a power law behavior, with an identical power law exponent (~0.16). Such power law behaviors, characteristic of a gel, were observed in various polymer networks (49), including biopolymers (50).

Megill et al. (12) measured the compressive stiffness of the mesoglea of *P. penicillatus* and found that the mean Young's modulus was ~340 Pa. An exact comparison with our macrorheological measurements is not possible, but a rough estimate can be made when considering the mesoglea as a purely elastic isotropic and incompressible material. The value of the elastic modulus G' would then be one-third of the Young's modulus: G' is ~110 Pa. Although we measured a smaller elastic modulus (~20 Pa at $\omega = 1$ rad/s) in *A. aurita*, the order of magnitude is in agreement with our measurements. The differences in the mechanical properties can be related to the differences in size and shape between *P. penicillatus* and *A. aurita*, leading to somewhat different fibrous organizations (15) and mechanical properties: *A. aurita* is an oblate jellyfish and *P. penicillatus* a jellyfish with a torpedo shape (12).

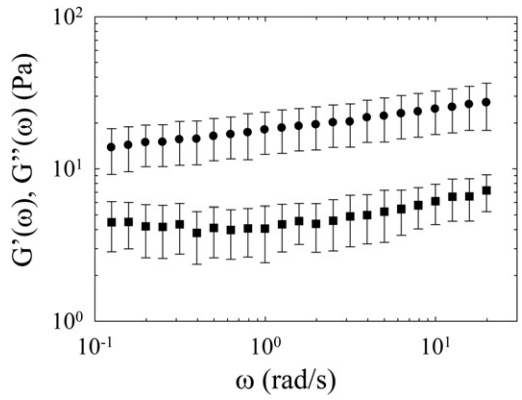

FIGURE 4 Macrorheological measurements. The frequency dependence of the averaged elastic (*circles*) and viscous (*squares*) moduli of mesoglea slices of adult jellyfish were obtained at the macroscopic scale using a shear rheometer. The average was performed over 18 different slices of mesoglea. (*Bars*) Standard deviation due to the dispersion of the measurements. At macroscopic scale, the mesoglea behaves like a viscoelastic gel.

Microrheology experiments

Microrheology experiments were performed on 30 juvenile jellyfish and 6 adult jellyfish. The microbeads were systematically injected in the same functional network region, characterized by the thick vertical fibers architecture far from the cellular sheets and tangential big fibers.

Juvenile jellyfish

Fig. 5 *A* shows the result from a typical experiment in the mesoglea of a juvenile jellyfish. The MSD as a function of the lag time for 11 different beads is represented. These beads were microinjected in the mesoglea and visualized one day after injection. The MSD is plotted in log-log scale and the local slopes of all curves are <1: the beads perform subdiffusive motions. This means that each bead probes a viscoelastic medium (45), which is consistent with macrorheological measurements. However, the most striking pattern is the diversity of microbeads behaviors: when viewing the specimen, they showed various Brownian motions. Some of them moved much more than others, as reflected by the diversity of MSD curves shown in Fig. 5 *A*; the higher MSD corresponded to the more mobile beads. These local variations of the microbeads behaviors implicate that the fine fiber network of the jellyfish ECM is very heterogeneous at the micron scale. This spatial heterogeneity is consistent with SEM observations (Fig. 3 *A*), revealing important local variations of the fibrous organization.

Adult jellyfish

Fig. 5 *B* shows the result from a typical experiment in the mesoglea of an adult jellyfish. The MSD as a function of the lag time for 13 different beads is represented. As observed in juvenile jellyfish, all the beads performed a subdiffusive motion, revealing a surrounding viscoelastic medium, and the MSD of the beads were drastically different from one probe to another. However, it should be noticed that the dispersion of the observed MSD is larger in the mesoglea of adult jellyfish than in juvenile ones. In the fibrous network of adult jellyfish, some of the beads show little Brownian motion; the MSD of these probes is very low ($<10^{-4}$ μm^2) and almost constant during time. It has been checked that their motions are above the resolution limit of the detection system. These beads were tightly trapped in the fibrous network and their MSD reflected the nearly purely elastic response of the cage in which they were embedded at the probe length-scale. The other beads moved more freely and their MSD are comparable to those observed in the mesoglea of juvenile jellyfish.

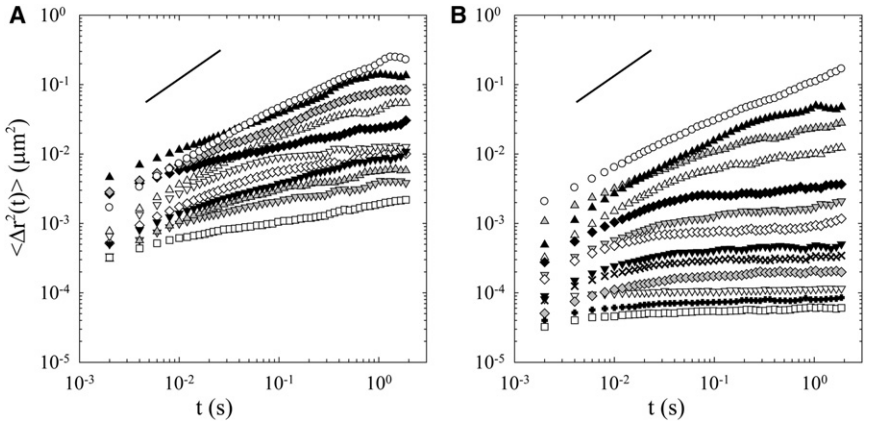

FIGURE 5 Microrheological measurements. Time-averaged MSD of 1-μm microbeads embedded in the mesogleal ECM as a function of the lag time. The microprobes were injected and visualized together and each symbol represents the MSD of a different microbead. (*Solid line* in each panel) Slope of 1. The dispersion of MSD curves shows that the fibrous network of jellyfish ECM is very heterogeneous at the micron scale. (*A*) MSD of microprobes injected in the mesoglea of a juvenile jellyfish. (*B*) MSD of microprobes injected in the mesoglea of an adult jellyfish. The dispersion of MSD curves is more important in adult jellyfish than in juvenile ones. Some of the beads enhance a very tiny Brownian motion. They explore stiff microenvironments of the ECM. The other beads move more freely and their MSD are comparable to those observed in the mesoglea of juvenile jellyfish.

Viscoelastic moduli at macro- and microscales

Macrorheology and microrheology experiments were performed in the mesoglea of adult jellyfish. To compare these rheological measurements performed at different scales, frequency-dependent viscoelastic moduli were calculated from the MSD of the beads, following Eq. 4 (see Material and Methods). Equation 4 has been established for a homogeneous medium, and $\langle \Delta r^2(1/\omega) \rangle$ should be evaluated by an average over the MSD of several beads, i.e., evaluated at $t = 1/\omega$. However, jellyfish ECM was highly heterogeneous as reflected by the dispersion of MSD curves (Fig. 5 *B*). In such heterogeneous medium, the dispersion of MSD reflects a dispersion of local viscoelastic moduli (34). Thus, $\langle \Delta r^2(1/\omega) \rangle$ was evaluated for each bead independently (34). However, $\langle \Delta r^2(1/\omega) \rangle$ was only calculated at short lag time ($t < 2$ s, $\omega > 3.14$ rad/s), so that the time-average is sufficient to maintain reliable statistics for the calculation of the viscoelastic moduli at the local microscale.

Fig. 6 shows the average viscoelastic moduli G' and G'' at macroscopic scale, placed in context with calculated G' and G'' at microscopic scale. G' and G'' at microscopic scale were calculated from the MSD of two different microbeads, showing very different behaviors: a first bead moving very little and a second one that was very mobile. In Fig. 5 *B*, the MSD of the bead moving very little (slow motion) was plotted with open squares and the MSD of the very mobile bead (fast motion) was plotted with open circles. The orders of magnitude of the elastic and viscous moduli measured with a shear rheometer were close to those calculated from the beads moving very little, tightly embedded in the fibrous network (Fig. 6). However, the more freely moving beads explored much softer microenvironments (with lower viscoelastic moduli). At a macroscopic scale, the mesoglea appeared to be stiffer than numerous microenvironments of its fibrous structure.

DISCUSSION

Rheological properties of jellyfish mesoglea were measured at different scales. We found that the ECM behaved as a viscoelastic gel at the macroscopic scale and as a much softer and heterogeneous viscoelastic structure at the microscopic scale. In addition, DIC microscopy techniques revealed the architecture of thick fibers traversing the ECM. SEM experiments showed that the small fibrils were randomly and heterogeneously distributed. Finally, we investigated the evolution of the microrheological properties of the ECM at different stages of jellyfish development and

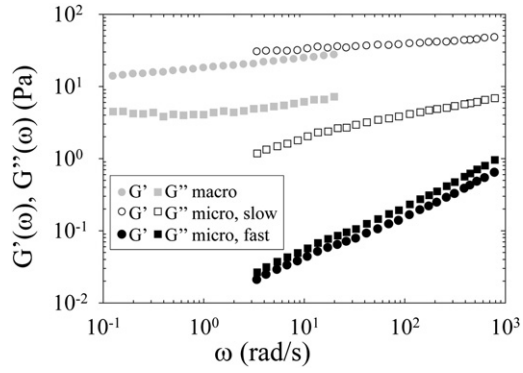

FIGURE 6 Viscoelastic moduli at macroscopic and microscopic scales. Viscoelastic moduli G' and G'' were obtained from macrorheology and microrheology experiments in adult jellyfish ECM. (*Circles*) G'; (*squares*) G''. (*Shaded symbols*) The moduli G' and G'' at macroscopic scale, obtained with a shear rheometer. G' and G'' at microscopic scale were calculated from the MSD curves of two different microbeads: a bead moving very little (slow) and a very mobile bead (fast). (*Open symbols*) G' and G'' calculated from the MSD of the probe that moved very little. (*Solid symbols*) G' and G'' calculated from the MSD of the very mobile bead. The different behaviors of these two beads correspond to different local viscoelastic moduli. The orders of magnitude of the elastic and viscous moduli measured with a shear rheometer are close to those calculated from the bead moving very little. The more freely moving bead explores a much softer microenvironment (with lower viscoelastic moduli).

measured that the ECM in adult jellyfish was locally stiffer than in juvenile ones.

Limitations of microrheology technique

We measured the mechanical properties of the mesoglea at the microscale by injecting microbeads in the jellyfish ECM and subsequently tracking their Brownian motion. The drawback of this technique is that the injection procedure is invasive and may damage locally the fibrous network. However, the Brownian motion of the microbeads was observed one day after injection. We measured that the Brownian motion of the microbeads was more constrained one day after injection than immediately after injection and remained similar at different time points during the subsequent four days. We interpret these results as a local embedding of each bead in the mesogleal fibrous network, occurring progressively, and well achieved one day after injection. We assume that during one day, the seawater injected with the beads could progressively diffuse, the ECM is restored locally, and the microbeads are embedded in the ECM. The advantage of this technique is that microbeads, introduced within the jellyfish, are put in contact with the ECM; its mechanical properties can then be probed directly and locally.

Mesoglea and collagen gels

The mesoglea gel of *A. aurita* is a fibrous system and is partly composed of collagen fibers. Collagen fibers in Cnidaria are found to resemble different vertebrate collagen types. Miura and Kimura (51) found chemically alike collagen Type V in the jellyfish *Stomolophus nomuria*. Analogs to collagen Type I, II, and IV were found in different species of hydra (9,52). To our knowledge, the collagen chains in *A. aurita* were not chemically identified.

Our macrorheological results on the ECM of *A. aurita* were similar to those obtained in Type-I reconstituted collagen gels (36,53,54). Their values of the viscoelastic moduli were in the same range as the values we measured. They likewise showed that the elastic modulus (G') was higher than the viscous one (G''), with G' increasing slightly with frequency. Furthermore, they found comparable power law behavior for viscoelastic moduli. Indeed, we measured in the mesoglea, between 1 and 20 rad/s, that G' and G'' increased with frequency with a power law exponent at ~0.16. This exponent is in the same range as power law exponents measured in Type-I reconstituted collagen gels in the same frequency domain: Knapp et al. (53) measured a power law exponent at ~0.13 and Velegol and Lanni (36) at ~0.15.

Velegol and Lanni (36) and Parekh and Velegol (55) also determined the elastic moduli of Type-I collagen gel at microscopic scale using laser trap microrheometry. They measured important variations in elastic moduli from position to position, revealing high heterogeneity of two orders of magnitude at micron scale. (Note that we have found, for the elastic component (G'), an even larger heterogeneity of three orders of magnitude for adult jellyfish (Fig. 6) and a somewhat smaller heterogeneity for juvenile jellyfish.

The fibrous system of the jellyfish mesoglea, however, is not composed only of collagen fibers, but also contains proteins such as fibrillin that form elastic fibers (12). Hsu et al. (54) measured the viscoelastic properties of collagen gels to which ~10% of elastic proteins (elastin) were added. At 25°C, they did not find a significant difference between elastin-containing gels and pure collagen gels. In all, from a rheological point of view, the mesoglea shows similarities with a simple collagen gel.

Mesoglea at macroscopic and microscopic scales

The mesogleal fibrous network is traversed by thick vertical fibers anchored in a three-dimensional network of fine fibrils as shown before by others (6–8,12,15) and as is shown in Figs. 2 and 3. Weber and Schmid (15) described the ECM of the mesoglea as a flexible foam mattress strengthened by vertical struts. Microrheology experiments primarily probe the mechanical properties of the fine fibrils meshwork, whereas macrorheology experiments measure the viscoelastic properties of the whole mesoglea, including the thick fibers. These experiments show that the network of fine fibrils is very soft and heterogeneous and that the stiffness of the mesoglea must be insured essentially by the architecture of thick fibers that structure the mesoglea. In contrast, for cellular migration and morphogenesis, the soft viscoelastic microenvironment plays likely a significant role.

Swimming and mesogleal deformations

In addition to maintaining the radial integrity, the thick vertical fibers also play a role during swimming. *A. aurita* swim with a combined jet-paddling mode of propulsion (17). During the contraction phase, the muscles located in the subumbrella contract predominantly circumferentially, which compress and shear the mesoglea in the plane perpendicular to the oral-aboral axis and elongate it along the oral-aboral axis (18). Although the mesogleal deformations during swimming are complex, the natural shearing plane during swimming corresponds to the shearing plane used in macrorheological experiments. At the frequency of muscle contractions (~1 rad/s), macrorheological results (Fig. 4) show that the mesoglea is much more elastic than viscous (G' is 10-times higher than G''). Although the microstructure contains viscous microenvironments (Fig. 6), the macrostructure is nearly purely elastic, which confirms (8,12,15,18) that the energy stored in the bell after muscle contractions can be released essentially elastically.

Aging of jellyfish ECM

Each contraction of the bell may cause a significant radial compression of the fibrous plexus, leading to a lengthening of the fiber network. The stress caused by repetitive muscular contractions progressively shapes the fibrous architecture of the ECM, leading to the formation of the thick vertical fibers architecture (15).

Observations of juvenile and adult jellyfish revealed indeed that the thick fibers are much thinner in juvenile jellyfish than in adult ones. In addition, SEM observations showed that thick fibers are woven together by the fine fibrils of the ECM (Fig. 3 *A*), which was also observed by Weber and Schmid (15). For reconstituted Type-I collagen gel it was shown that collagen fibers align along tensional stresses (55,56), set out at the fibril level, after which they gradually form larger fibers. These results suggest that during aging of the jellyfish ECM, the fine meshwork of fibrils progressively aggregates and forms thick fibers, which thicken gradually with time.

In our microrheology experiments, beads probing stiff microenvironments in adult jellyfish must be trapped between densely packed thick fibers. The other beads move more freely in the ECM and their MSD are very similar in adult and juvenile jellyfish. It seems that these more freely moving beads explore microenvironments in the loose mesh of fine fibers that are not aggregated. The progressive stiffening of the ECM occurring at microscopic scale is assumed to reflect the aging of the jellyfish mesoglea.

Furthermore, no differences in the microrheology results of the juvenile jellyfish could be observed when ECM was probed with the microbeads up to four days of swimming after injection. This implies that mechanical stiffening of the microenvironments due to the gradual intertwining of the fibers is significantly observable at long timescales, likely in the order of several weeks.

CONCLUSION

The rheological properties of the ECM of the jellyfish mesoglea were measured at macroscopic and microscopic scales. Whereas the ECM behaved as a viscoelastic gel at the macroscopic scale, it proved to be a much softer and heterogeneous viscoelastic structure at the cellular scale, the scale at which morphogenetic processes occur. The fibrous architecture of the mesoglea observed by differential interference contrast and scanning electron microscopy was in agreement with our measurements of the mechanical properties of the ECM at macroscopic and microscopic scales.

Formation of this fiber network architecture proved to be a dynamical process: microrheology experiments performed on juvenile and adult jellyfish revealed a progressive stiffening of microenvironments in the ECM by a gradual aggregation of fibers. This aggregation of fibers is likely to be enhanced by the repetitive muscular contractions of the jellyfish, shaping the fibrous architecture of the ECM progressively during aging.

SUPPORTING MATERIAL

Details of the injection and microrheology experimental procedure, control experiments, and three figures are available at http://www.biophysj.org/biophysj/supplemental/S0006-3495(11)05355-0.

The authors thank David Montero for the SEM images in Fig. 3, *A* and *B*, Matthieu Receveur for his technical help, and Nicolas Cagnon, Pierre-Yves Bouis, and the team from La Cité de la Mer in Cherbourg, France, who taught us how to rear jellyfish.

This work was supported by grants (Programme Interdisciplinaire de Recherche and Projet Exploratoire) from the Centre National de la Recherche Scientifique and by a grant (Bonus Qualité Recherche) from the University Paris Diderot.

REFERENCES

1. Discher, D. E., P. Janmey, and Y. L. Wang. 2005. Tissue cells feel and respond to the stiffness of their substrate. *Science* 310:1139–1143.
2. Saez, A., M. Ghibaudo, …, B. Ladoux. 2007. Rigidity-driven growth and migration of epithelial cells on microstructured anisotropic substrates. *Proc. Natl. Acad. Sci. USA* 104:8281–8286.
3. Baker, E. L., R. T. Bonnecaze, and M. H. Zaman. 2009. Extracellular matrix stiffness and architecture govern intracellular rheology in cancer. *Biophys. J.* 97:1013–1021.
4. Levental, I., P. C. Georges, and P. A. Janmey. 2007. Soft biological materials and their impact on cell function. *Soft Matter* 3:299–306.
5. Ingber, D. E. 2002. Mechanical signaling and the cellular response to extracellular matrix in angiogenesis and cardiovascular physiology. *Circ. Res.* 91:877–887.
6. Bouillon, J., and G. Coppois. 1977. Comparative-study of mesoglea of cnidarians. *Cah. Biol. Mar.* 18:339–368.
7. Chapman, G. 1953. Studies of the mesoglea of coelenterates. 1. Histology and chemical properties. *Q. J. Microsc. Sci.* 94:155–176.
8. Chapman, G. 1959. The mesoglea of *Pelagia noctiluca*. *Q. J. Microsc. Sci.* 100:599–610.
9. Shimizu, H., R. Aufschnaiter, …, X. Zhang. 2008. The extracellular matrix of hydra is a porous sheet and contains type IV collagen. *Zoology (Jena)* 111:410–418.
10. Russel, F. S. 1970. The Medusae of the British Isles. Vol. II. Pelagic Scyphozoa, with a supplement to Vol. I. Cambridge University Press, London, UK.
11. Reber-Müller, S., T. Spissinger, …, V. Schmid. 1995. An extracellular matrix protein of jellyfish homologous to mammalian fibrillins forms different fibrils depending on the life stage of the animal. *Dev. Biol.* 169:662–672.
12. Megill, W. M., J. M. Gosline, and R. W. Blake. 2005. The modulus of elasticity of fibrillin-containing elastic fibers in the mesoglea of the hydromedusa *Polyorchis penicillatus*. *J. Exp. Biol.* 208:3819–3834.
13. Shaposhnikova, T., I. Matveev, …, O. Podgornaya. 2005. Mesogleal cells of the jellyfish *Aurelia aurita* are involved in the formation of mesogleal fibers. *Cell Biol. Int.* 29:952–958.
14. Denton, E. J. 1963. Buoyancy mechanisms of sea creatures. *Endeavour* 22:3–8.
15. Weber, C., and V. Schmid. 1985. The fibrous system in the extracellular matrix of hydromedusae. *Tissue Cell* 17:811–822.

16. Nawroth, J. C., K. E. Feitl, …, J. O. Dabiri. 2010. Phenotypic plasticity in juvenile jellyfish medusae facilitates effective animal-fluid interaction. *Biol. Lett.* 6:389–393.

17. Dabiri, J. O., S. P. Colin, and J. H. Costello. 2007. Morphological diversity of medusan lineages constrained by animal-fluid interactions. *J. Exp. Biol.* 210:1868–1873.

18. Gladfelt, W. B. 1972. Structure and function of locomotory system of *Polyorchis montereyensis* (Cnidaria, Hydrozoa). *Helgol. Wiss. Meeresunters.* 23:38–79.

19. Schmid, V., A. Bally, …, C. Weber. 1991. The extracellular matrix (mesoglea) of hydrozoan jellyfish and its ability to support cell-adhesion and spreading. *Hydrobiologia* 216:3–10.

20. Sarras, Jr., M. P., X. M. Zhang, …, D. R. Abrahamson. 1993. Extracellular matrix (mesoglea) of *Hydra vulgaris* III. Formation and function during morphogenesis of hydra cell aggregates. *Dev. Biol.* 157:383–398.

21. Frank, U., and B. Rinkevich. 1999. Scyphozoan jellyfish's mesoglea supports attachment, spreading and migration of anthozoans' cells in vitro. *Cell Biol. Int.* 23:307–311.

22. Shimizu, H., X. M. Zhang, …, M. P. Sarras, Jr. 2002. Epithelial morphogenesis in hydra requires de novo expression of extracellular matrix components and matrix metalloproteinases. *Development* 129:1521–1532.

23. Kleinman, H. K., D. Philp, and M. P. Hoffman. 2003. Role of the extracellular matrix in morphogenesis. *Curr. Opin. Biotechnol.* 14:526–532.

24. Tucker, R. P., B. Shibata, and T. N. Blankenship. 2011. Ultrastructure of the mesoglea of the sea anemone *Nematostella vectensis* (*Edwardsiidae*). *Invertebr. Biol.* 130:11–24.

25. Alexander, R. M. 1964. Viscoelastic properties of mesoglea of jellyfish. *J. Exp. Biol.* 41:363–369.

26. MacKintosh, F. C., and C. F. Schmidt. 1999. Microrheology. *Curr. Opin. Colloid Interface Sci.* 4:300–307.

27. Breedveld, V., and D. J. Pine. 2003. Microrheology as a tool for high-throughput screening. *J. Mater. Sci.* 38:4461–4470.

28. Abou, B., C. Gay, …, S. Gorb. 2010. Extensive collection of femtoLiter pad secretion droplets in the beetle *Leptinotarsa decemlineata* allows nanoliter microrheology. *J. R. Soc. Interface* 7:1745–1752.

29. Weihs, D., T. G. Mason, and M. A. Teitell. 2006. Bio-microrheology: a frontier in microrheology. *Biophys. J.* 91:4296–4305.

30. Massiera, G., K. M. Van Citters, …, J. C. Crocker. 2007. Mechanics of single cells: rheology, time dependence, and fluctuations. *Biophys. J.* 93:3703–3713.

31. Daniels, B. R., C. M. Hale, …, D. Wirtz. 2010. Differences in the microrheology of human embryonic stem cells and human induced pluripotent stem cells. *Biophys. J.* 99:3563–3570.

32. Fabry, B., G. N. Maksym, …, J. J. Fredberg. 2001. Scaling the microrheology of living cells. *Phys. Rev. Lett.* 87:148102.

33. Valentine, M. T., P. D. Kaplan, …, D. A. Weitz. 2001. Investigating the microenvironments of inhomogeneous soft materials with multiple particle tracking. *Phys. Rev. E* 64:061506.

34. Tseng, Y., T. P. Kole, and D. Wirtz. 2002. Micromechanical mapping of live cells by multiple-particle-tracking microrheology. *Biophys. J.* 83:3162–3176.

35. Ziemann, F., J. Rädler, and E. Sackmann. 1994. Local measurements of viscoelastic moduli of entangled actin networks using an oscillating magnetic bead micro-rheometer. *Biophys. J.* 66:2210–2216.

36. Velegol, D., and F. Lanni. 2001. Cell traction forces on soft biomaterials. I. Microrheology of type I collagen gels. *Biophys. J.* 81:1786–1792.

37. Mason, T. G., and D. A. Weitz. 1995. Optical measurements of frequency-dependent linear viscoelastic moduli of complex fluids. *Phys. Rev. Lett.* 74:1250–1253.

38. Palmer, A., J. Xu, …, D. Wirtz. 1999. Diffusing wave spectroscopy microrheology of actin filament networks. *Biophys. J.* 76:1063–1071.

39. Mason, T. G. 2000. Estimating the viscoelastic moduli of complex fluids using the generalized Stokes-Einstein equation. *Rheol. Acta* 39:371–378.

40. Kroiher, M., B. Siefker, and S. Berking. 2000. Induction of segmentation in polyps of *Aurelia aurita* (Scyphozoa, Cnidaria) into medusae and formation of mirror-image medusa anlagen. *Int. J. Dev. Biol.* 44:485–490.

41. Chapman, D. M. 1999. Microanatomy of the bell rim of *Aurelia aurita* (Cnidaria: Scyphozoa). *Can. J. Zool. Revue Can. Zool.*. 77:34–46.

42. Litke, L. L., and F. N. Low. 1977. Fixative tonicity for scanning electron microscopy of delicate chick embryos. *Am. J. Anat.* 121–127.

43. Rasband, W. S. 1997–2007 ImageJ. US National Institutes of Health, Bethesda, MD. http://rsb.info.nih.gov/ij/. (Source code for the plug-in is available at http://www.msc.univparis.diderot.fr/~olivier/ImageJ/; tracker_Install.zip; 29/03/2009)

44. Weber, C., E. Kurz, and V. Schmid. 1987. The fibrous system of the extracellular matrix of *Podocoryne carnea* and its degradation by the subumbrellar plate endoderm demonstrated by a monoclonal antibody. *Tissue Cell.* 19:757–771.

45. Dasgupta, B. R., and D. A. Weitz. 2005. Microrheology of cross-linked polyacrylamide networks. *Phys. Rev. E* 71:021504.

46. Dasgupta, B. R., S. Y. Tee, …, D. A. Weitz. 2002. Microrheology of polyethylene oxide using diffusing wave spectroscopy and single scattering. *Phys. Rev. E* 65:051505.

47. Parry, D. A. D., and A. S. Craig. 1977. Quantitative electron microscope observations of the collagen fibrils in rat-tail tendon. *Biopolymers* 16:1015–1031.

48. Raub, C. B., V. Suresh, …, S. C. George. 2007. Noninvasive assessment of collagen gel microstructure and mechanics using multiphoton microscopy. *Biophys. J.* 92:2212–2222.

49. Warlus, S., and A. Ponton. 2009. A new interpretation for the dynamic behavior of complex fluids at the sol-gel transition using the fractional calculus. *Rheol. Acta* 48:51–58.

50. Rodd, A. B., J. Cooper-White, …, D. V. Boger. 2001. Gel point studies for chemically modified biopolymer networks using small amplitude oscillatory rheometry. *Polymer (Guildf.)* 42:185–198.

51. Miura, S., and S. Kimura. 1985. Jellyfish mesoglea collagen—characterization of molecules as α1-α2-α3 heterotrimers. *J. Biol. Chem.* 260:5352–5356.

52. Deutzmann, R., S. Fowler, …, M. P. Sarras, Jr. 2000. Molecular, biochemical and functional analysis of a novel and developmentally important fibrillar collagen (Hcol-I) in hydra. *Development* 127:4669–4680.

53. Knapp, D. M., V. H. Barocas, …, R. T. Tranquillo. 1997. Rheology of reconstituted type I collagen gel in confined compression. *J. Rheol.* 41:971–993.

54. Hsu, S., A. M. Jamieson, and J. Blackwell. 1994. Viscoelastic studies of extracellular matrix interactions in a model native collagen gel system. *Biorheology* 31:21–36.

55. Parekh, A., and D. Velegol. 2007. Collagen gel anisotropy measured by 2-D laser trap microrheometry. *Ann. Biomed. Eng.* 35:1231–1246.

56. Vader, D., A. Kabla, …, L. Mahadevan. 2009. Strain-induced alignment in collagen gels. *PLoS ONE* 4:e5902.